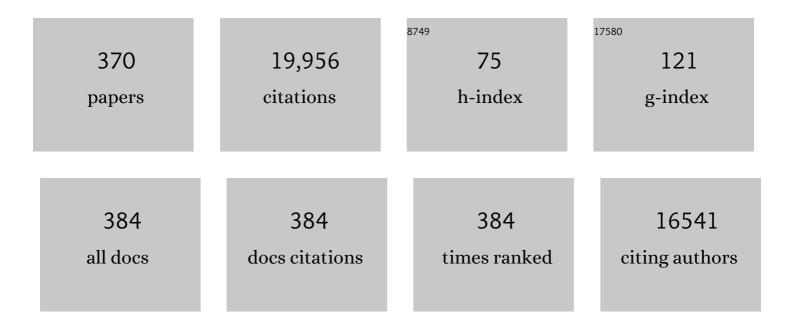
## Hiromi Yamashita

List of Publications by Year in descending order

Source: https://exaly.com/author-pdf/8041165/publications.pdf Version: 2024-02-01



#	Article	IF	CITATIONS
1	Photocatalytic Reduction of CO2with H2O on Titanium Oxides Anchored within Micropores of Zeolites:Â Effects of the Structure of the Active Sites and the Addition of Pt. Journal of Physical Chemistry B, 1997, 101, 2632-2636.	1.2	395
2	Pd and Pd–Ag Nanoparticles within a Macroreticular Basic Resin: An Efficient Catalyst for Hydrogen Production from Formic Acid Decomposition. ACS Catalysis, 2013, 3, 1114-1119.	5.5	339
3	Surfactantâ€Free Nonaqueous Synthesis of Plasmonic Molybdenum Oxide Nanosheets with Enhanced Catalytic Activity for Hydrogen Generation from Ammonia Borane under Visible Light. Angewandte Chemie - International Edition, 2014, 53, 2910-2914.	7.2	334
4	Enhanced visible-light-driven photocatalytic inactivation of Escherichia coli using g-C3N4/TiO2 hybrid photocatalyst synthesized using a hydrothermal-calcination approach. Water Research, 2015, 86, 17-24.	5.3	323
5	Ru and Ru–Ni Nanoparticles on TiO <sub>2</sub> Support as Extremely Active Catalysts for Hydrogen Production from Ammonia–Borane. ACS Catalysis, 2016, 6, 3128-3135.	5.5	310
6	Superhydrophobic Surfaces with Photocatalytic Selfâ€Cleaning Properties by Nanocomposite Coating of TiO <sub>2</sub> and Polytetrafluoroethylene. Advanced Materials, 2012, 24, 3697-3700.	11.1	298
7	Photocatalytic Reduction of CO2 with H2O on Tiâ <sup>^^</sup> î² Zeolite Photocatalysts:  Effect of the Hydrophobic and Hydrophilic Properties. Journal of Physical Chemistry B, 2001, 105, 8350-8355.	1.2	287
8	Photocatalytic reduction of CO2 with H2O on various titanium oxide photocatalysts. RSC Advances, 2012, 2, 3165.	1.7	286
9	Charge Carrier Dynamics of Standard TiO2Catalysts Revealed by Femtosecond Diffuse Reflectance Spectroscopy. Journal of Physical Chemistry B, 1999, 103, 3120-3127.	1.2	269
10	Selective formation of CH3OH in the photocatalytic reduction of CO2 with H2O on titanium oxides highly dispersed within zeolites and mesoporous molecular sieves. Catalysis Today, 1998, 45, 221-227.	2.2	251
11	Metal–organic framework-based nanomaterials for adsorption and photocatalytic degradation of gaseous pollutants: recent progress and challenges. Environmental Science: Nano, 2019, 6, 1006-1025.	2.2	245
12	In-Situ XAFS, Photoluminescence, and IR Investigations of Copper Ions Included within Various Kinds of Zeolites. Structure of Cu(I) Ions and Their Interaction with CO Molecules. The Journal of Physical Chemistry, 1996, 100, 397-402.	2.9	242
13	Photocatalytic Decomposition of NO at 275 K on Titanium Oxides Included within Y-Zeolite Cavities:Â The Structure and Role of the Active Sites. The Journal of Physical Chemistry, 1996, 100, 16041-16044.	2.9	242
14	Preparation of Titanium Oxide Photocatalysts Anchored on Porous Silica Glass by a Metal Ion-Implantation Method and Their Photocatalytic Reactivities for the Degradation of 2-Propanol Diluted in Water. Journal of Physical Chemistry B, 1998, 102, 10707-10711.	1.2	232
15	Design of unique titanium oxide photocatalysts by an advanced metal ion-implantation method and photocatalytic reactions under visible light irradiation. Research on Chemical Intermediates, 1998, 24, 143-149.	1.3	230
16	The Synthesis of Size―and Colorâ€Controlled Silver Nanoparticles by Using Microwave Heating and their Enhanced Catalytic Activity by Localized Surface Plasmon Resonance. Angewandte Chemie - International Edition, 2013, 52, 7446-7450.	7.2	225
17	Isolated Single-Atomic Ru Catalyst Bound on a Layered Double Hydroxide for Hydrogenation of CO <sub>2</sub> to Formic Acid. ACS Catalysis, 2017, 7, 3147-3151.	5.5	225
18	Dramatic Enhancement of CO <sub>2</sub> Uptake by Poly(ethyleneimine) Using Zirconosilicate Supports. Journal of the American Chemical Society, 2012, 134, 10757-10760.	6.6	205

#	Article	IF	CITATIONS
19	Surface Engineering of a Supported PdAg Catalyst for Hydrogenation of CO <sub>2</sub> to Formic Acid: Elucidating the Active Pd Atoms in Alloy Nanoparticles. Journal of the American Chemical Society, 2018, 140, 8902-8909.	6.6	202
20	Hydrogen Doped Metal Oxide Semiconductors with Exceptional and Tunable Localized Surface Plasmon Resonances. Journal of the American Chemical Society, 2016, 138, 9316-9324.	6.6	201
21	Amine-functionalized MIL-101(Cr) with imbedded platinum nanoparticles as a durable photocatalyst for hydrogen production from water. Chemical Communications, 2014, 50, 11645-11648.	2.2	199
22	Catalytic Transfer Hydrogenation of Biomass-Derived Levulinic Acid and Its Esters to γ-Valerolactone over Sulfonic Acid-Functionalized UiO-66. ACS Sustainable Chemistry and Engineering, 2017, 5, 1141-1152.	3.2	198
23	Functionalized mesoporous SBA-15 silica: recent trends and catalytic applications. Nanoscale, 2020, 12, 11333-11363.	2.8	193
24	Amine-Functionalized MIL-125 with Imbedded Palladium Nanoparticles as an Efficient Catalyst for Dehydrogenation of Formic Acid at Ambient Temperature. Journal of Physical Chemistry C, 2013, 117, 22805-22810.	1.5	188
25	Characterization of Titaniumâ^'Silicon Binary Oxide Catalysts Prepared by the Solâ^'Gel Method and Their Photocatalytic Reactivity for the Liquid-Phase Oxidation of 1-Octanol. Journal of Physical Chemistry B, 1998, 102, 5870-5875.	1.2	184
26	Title is missing!. Catalysis Letters, 2000, 67, 135-137.	1.4	180
27	Plasmonic Au@Pd Nanoparticles Supported on a Basic Metal–Organic Framework: Synergic Boosting of H <sub>2</sub> Production from Formic Acid. ACS Energy Letters, 2017, 2, 1-7.	8.8	180
28	Single-site and nano-confined photocatalysts designed in porous materials for environmental uses and solar fuels. Chemical Society Reviews, 2018, 47, 8072-8096.	18.7	176
29	A Plasmonic Molybdenum Oxide Hybrid with Reversible Tunability for Visibleâ€Lightâ€Enhanced Catalytic Reactions. Advanced Materials, 2015, 27, 4616-4621.	11.1	174
30	Design and architecture of metal organic frameworks for visible light enhanced hydrogen production. Applied Catalysis B: Environmental, 2017, 218, 555-569.	10.8	173
31	Twoâ€Phase System Utilizing Hydrophobic Metal–Organic Frameworks (MOFs) for Photocatalytic Synthesis of Hydrogen Peroxide. Angewandte Chemie - International Edition, 2019, 58, 5402-5406.	7.2	169
32	Influence of char surface chemistry on the reduction of nitric oxide with chars. Energy & Fuels, 1993, 7, 85-89.	2.5	166
33	Photocatalytic Degradation of 1-Octanol on Anchored Titanium Oxide and on TiO2Powder Catalysts. Journal of Catalysis, 1996, 158, 97-101.	3.1	161
34	PdAg Nanoparticles Supported on Functionalized Mesoporous Carbon: Promotional Effect of Surface Amine Groups in Reversible Hydrogen Delivery/Storage Mediated by Formic Acid/CO <sub>2</sub> . ACS Catalysis, 2018, 8, 2277-2285.	5.5	157
35	Photocatalytic decomposition of NO at 275 K on titanium oxide catalysts anchored within zeolite cavities and framework. Applied Surface Science, 1997, 121-122, 305-309.	3.1	148
36	Graphene Coating of TiO <sub>2</sub> Nanoparticles Loaded on Mesoporous Silica for Enhancement of Photocatalytic Activity. Journal of Physical Chemistry C, 2010, 114, 15049-15053.	1.5	147

#	Article	IF	CITATIONS
37	A Visibleâ€Lightâ€Harvesting Assembly with a Sulfocalixarene Linker between Dyes and a Ptâ€TiO <sub>2</sub> Photocatalyst. Angewandte Chemie - International Edition, 2013, 52, 916-919.	7.2	139
38	Catalytic transfer hydrogenation of biomass-derived levulinic acid and its esters to γ-valerolactone over ZrO 2 catalyst supported on SBA-15 silica. Catalysis Today, 2017, 281, 418-428.	2.2	129
39	Harnessing single-active plasmonic nanostructures for enhanced photocatalysis under visible light. Journal of Materials Chemistry A, 2015, 3, 5244-5258.	5.2	127
40	Relationship between the Local Structures of Titanium Oxide Photocatalysts and Their Reactivities in the Decomposition of NO. Journal of Physical Chemistry B, 2001, 105, 8395-8398.	1.2	126
41	Enhancement of the Photoinduced Oxidation Activity of a Ruthenium(II) Complex Anchored on Silica oated Silver Nanoparticles by Localized Surface Plasmon Resonance. Angewandte Chemie - International Edition, 2010, 49, 8598-8601.	7.2	126
42	Preparation of Hydroxynaphthalene-Modified TiO <sub>2</sub> via Formation of Surface Complexes and their Applications in the Photocatalytic Reduction of Nitrobenzene under Visible-Light Irradiation. ACS Applied Materials & Interfaces, 2012, 4, 6635-6639.	4.0	125
43	Photocatalytic reactions on chromium containing mesoporous silica molecular sieves (Cr-HMS) under visible light irradiation: decomposition of NO and partial oxidation of propane. Chemical Communications, 2001, , 435-436.	2.2	123
44	Applications of Single-site Photocatalysts Implanted within the Silica Matrixes of Zeolite and Mesoporous Silica. Chemistry Letters, 2007, 36, 348-353.	0.7	120
45	Reaction of nitric oxide with metal-loaded carbon in the presence of oxygen. Applied Catalysis, 1991, 78, L1-L6.	1.1	119
46	Efficient photocatalytic degradation of organics diluted in water and air using TiO <sub>2</sub> designed with zeolites and mesoporous silica materials. Journal of Materials Chemistry, 2011, 21, 2407-2416.	6.7	119
47	A novel conversion process for waste slag: synthesis of a hydrotalcite-like compound and zeolite from blast furnace slag and evaluation of adsorption capacities. Journal of Materials Chemistry, 2010, 20, 5052.	6.7	118
48	Enhanced CO <sub>2</sub> Adsorption over Polymeric Amines Supported on Heteroatomâ€Incorporated SBAâ€15 Silica: Impact of Heteroatom Type and Loading on Sorbent Structure and Adsorption Performance. Chemistry - A European Journal, 2012, 18, 16649-16664.	1.7	118
49	Local structures and photocatalytic reactivities of the titanium oxide and chromium oxide species incorporated within micro- and mesoporous zeolite materials: XAFS and photoluminescence studies. Current Opinion in Solid State and Materials Science, 2003, 7, 471-481.	5.6	116
50	Design and Functionalization of Photocatalytic Systems within Mesoporous Silica. ChemSusChem, 2014, 7, 1528-1536.	3.6	109
51	Hydrogen spillover-driven synthesis of high-entropy alloy nanoparticles as a robust catalyst for CO2 hydrogenation. Nature Communications, 2021, 12, 3884.	5.8	109
52	Phenylamine-functionalized mesoporous silica supported PdAg nanoparticles: a dual heterogeneous catalyst for formic acid/CO <sub>2</sub> -mediated chemical hydrogen delivery/storage. Chemical Communications, 2017, 53, 4677-4680.	2.2	107
53	Recent strategies targeting efficient hydrogen production from chemical hydrogen storage materials over carbon-supported catalysts. NPG Asia Materials, 2018, 10, 277-292.	3.8	104
54	Mechanism of Photooxidation of Alcohol over Nb <sub>2</sub> O <sub>5</sub> . Journal of Physical Chemistry C, 2009, 113, 18713-18718.	1.5	102

#	Article	IF	CITATIONS
55	Synergic Catalysis of PdCu Alloy Nanoparticles within a Macroreticular Basic Resin for Hydrogen Production from Formic Acid. Chemistry - A European Journal, 2015, 21, 12085-12092.	1.7	102
56	Synthesis of Ce ions doped metal–organic framework for promoting catalytic H <sub>2</sub> production from ammonia borane under visible light irradiation. Journal of Materials Chemistry A, 2015, 3, 14134-14141.	5.2	102
57	Mild Deoxygenation of Sulfoxides over Plasmonic Molybdenum Oxide Hybrid with Dramatic Activity Enhancement under Visible Light. Journal of the American Chemical Society, 2018, 140, 9203-9210.	6.6	102
58	TiO2 photocatalyst for degradation of organic compounds in water and air supported on highly hydrophobic FAU zeolite: Structural, sorptive, and photocatalytic studies. Journal of Catalysis, 2012, 285, 223-234.	3.1	101
59	Pd Nanoparticles and Aminopolymers Confined in Hollow Silica Spheres as Efficient and Reusable Heterogeneous Catalysts for Semihydrogenation of Alkynes. ACS Catalysis, 2019, 9, 1993-2006.	5.5	101
60	Enhancement of plasmonic activity by Pt/Ag bimetallic nanocatalyst supported on mesoporous silica in the hydrogen production from hydrogen storage material. Applied Catalysis B: Environmental, 2018, 223, 10-15.	10.8	97
61	Hydrophobic Modification of a Mesoporous Silica Surface Using a Fluorine-Containing Silylation Agent and Its Application as an Advantageous Host Material for the TiO <sub>2</sub> Photocatalyst. Journal of Physical Chemistry C, 2009, 113, 1552-1559.	1.5	96
62	Enhanced Catalytic Activity on Titanosilicate Molecular Sieves Controlled by Cationâ^'Ï€ Interactions. Journal of the American Chemical Society, 2011, 133, 12462-12465.	6.6	96
63	Pd/Ag and Pd/Au bimetallic nanocatalysts on mesoporous silica for plasmon-mediated enhanced catalytic activity under visible light irradiation. Journal of Materials Chemistry A, 2016, 4, 10142-10150.	5.2	95
64	Title is missing!. Topics in Catalysis, 2002, 18, 95-100.	1.3	94
65	High-surface-area plasmonic MoO <sub>3â^'x</sub> : rational synthesis and enhanced ammonia borane dehydrogenation activity. Journal of Materials Chemistry A, 2017, 5, 8946-8953.	5.2	94
66	New Approaches Toward the Hydrogen Production From Formic Acid Dehydrogenation Over Pd-Based Heterogeneous Catalysts. Frontiers in Materials, 2019, 6, .	1.2	93
67	Shape and Composition Effects on Photocatalytic Hydrogen Production for Pt–Pd Alloy Cocatalysts. ACS Applied Materials & Interfaces, 2016, 8, 20667-20674.	4.0	91
68	A hydrophobic titanium doped zirconium-based metal organic framework for photocatalytic hydrogen peroxide production in a two-phase system. Journal of Materials Chemistry A, 2020, 8, 1904-1910.	5.2	89
69	Synthesis and characterization of FePd magnetic nanoparticles modified with chiral BINAP ligand as a recoverable catalyst vehicle for the asymmetric coupling reaction. Physical Chemistry Chemical Physics, 2009, 11, 8949.	1.3	88
70	Non-Noble-Metal Nanoparticle Supported on Metal–Organic Framework as an Efficient and Durable Catalyst for Promoting H <sub>2</sub> Production from Ammonia Borane under Visible Light Irradiation. ACS Applied Materials & Interfaces, 2016, 8, 21278-21284.	4.0	88
71	Synthesis and characterization of a Pd/Ag bimetallic nanocatalyst on SBA-15 mesoporous silica as a plasmonic catalyst. Journal of Materials Chemistry A, 2015, 3, 18889-18897.	5.2	87
72	Catalytically active, magnetically separable, and water-soluble FePt nanoparticles modified with cyclodextrin for aqueous hydrogenation reactions. Green Chemistry, 2009, 11, 1337.	4.6	83

#	Article	IF	CITATIONS
73	Synthesis of Tris(2,2â€~-bipyridine)iron(II) Complexes in Zeolite Y Cages:  Influence of Exchanged Alkali Metal Cations on Physicochemical Properties and Catalytic Activity. Journal of Physical Chemistry C, 2008, 112, 2593-2600.	1.5	81
74	Photocatalytic production of hydrogen peroxide through selective two-electron reduction of dioxygen utilizing amine-functionalized MIL-125 deposited with nickel oxide nanoparticles. Chemical Communications, 2018, 54, 9270-9273.	2.2	81
75	Controlled Pyrolysis of Niâ€MOFâ€74 as a Promising Precursor for the Creation of Highly Active Ni Nanocatalysts in Sizeâ€Selective Hydrogenation. Chemistry - A European Journal, 2018, 24, 898-905.	1.7	78
76	A pH-Induced Size Controlled Deposition of Colloidal Ag Nanoparticles on Alumina Support for Catalytic Application. Journal of Physical Chemistry C, 2009, 113, 16850-16854.	1.5	77
77	Esterification of levulinic acid with ethanol over sulfated mesoporous zirconosilicates: Influences of the preparation conditions on the structural properties and catalytic performances. Catalysis Today, 2014, 237, 18-28.	2.2	75
78	Enhanced hydrogen production from ammonia borane using controlled plasmonic performance ofÂAu nanoparticles deposited on TiO <sub>2</sub> . Journal of Materials Chemistry A, 2017, 5, 21883-21892.	5.2	75
79	A novel conversion process for waste slag: synthesis of calcium silicate hydrate from blast furnace slag and its application as a versatile adsorbent for water purification. Journal of Materials Chemistry A, 2013, 1, 7199.	5.2	72
80	Localized Surface Plasmon Resonances in Plasmonic Molybdenum Tungsten Oxide Hybrid for Visible-Light-Enhanced Catalytic Reaction. Journal of Physical Chemistry C, 2017, 121, 23531-23540.	1.5	72
81	The Local Structures of Silver(I) Ion Catalysts Anchored within Zeolite Cavities and Their Photocatalytic Reactivities for the Elimination of N2O into N2 and O2. Journal of Physical Chemistry B, 2004, 108, 2128-2133.	1.2	71
82	Enhanced photocatalytic properties of TiO <sub>2</sub> -loaded porous silica with hierarchical macroporous and mesoporous architectures in water purification. Journal of Materials Chemistry A, 2015, 3, 2323-2330.	5.2	70
83	Colorâ€Controlled Ag Nanoparticles and Nanorods within Confined Mesopores: Microwaveâ€Assisted Rapid Synthesis and Application in Plasmonic Catalysis under Visibleâ€Light Irradiation. Chemistry - A European Journal, 2015, 21, 11885-11893.	1.7	69
84	Characterization of Vanadium Oxide/ZSM-5 Zeolite Catalysts Prepared by the Solid-State Reaction and Their Photocatalytic Reactivity:  In Situ Photoluminescence, XAFS, ESR, FT-IR, and UVâ^'vis Investigations. Journal of Physical Chemistry B, 1998, 102, 5590-5594.	1.2	68
85	A new catalytic opportunity for waste materials: Application of waste slag based catalyst in CO2 fixation reaction. Journal of CO2 Utilization, 2013, 1, 50-59.	3.3	68
86	Design of TiO2-zeolite composites with enhanced photocatalytic performances under irradiation of UV and visible light. Microporous and Mesoporous Materials, 2013, 165, 142-147.	2.2	67
87	Design of macroporous TiO2 thin film photocatalysts with enhanced photofunctional properties. Energy and Environmental Science, 2011, 4, 1411.	15.6	66
88	Surface plasmon resonance enhancement of production of H2 from ammonia borane solution with tunable Cu2â °xS nanowires decorated by Pd nanoparticles. Nano Energy, 2017, 31, 57-63.	8.2	65
89	Fabrication of hydrophobic zeolites using triethoxyfluorosilane and their application as supports for TiO2 photocatalysts. Chemical Communications, 2008, , 4783.	2.2	63
90	New Route for the Preparation of Pd and PdAu Nanoparticles Using Photoexcited Ti-Containing Zeolite as an Efficient Support Material and Investigation of Their Catalytic Properties. Langmuir, 2009, 25, 11180-11187.	1.6	63

#	Article	IF	CITATIONS
91	Transesterifications using a hydrocalumite synthesized from waste slag: an economical and ecological route for biofuel production. Catalysis Science and Technology, 2012, 2, 1842.	2.1	63
92	Hybrid phase 1T/2H-MoS <sub>2</sub> with controllable 1T concentration and its promoted hydrogen evolution reaction. Nanoscale, 2020, 12, 11908-11915.	2.8	62
93	Progress in design and architecture of metal nanoparticles for catalytic applications. Physical Chemistry Chemical Physics, 2010, 12, 14420.	1.3	61
94	Highly efficient Ru/carbon catalysts prepared by pyrolysis of supported Ru complex towards the hydrogen production from ammonia borane. Applied Catalysis A: General, 2016, 527, 45-52.	2.2	61
95	Evolution of the PVP–Pd Surface Interaction in Nanoparticles through the Case Study of Formic Acid Decomposition. Langmuir, 2016, 32, 12110-12118.	1.6	61
96	Nitrogen-doped carbon materials as a promising platform toward the efficient catalysis for hydrogen generation. Applied Catalysis A: General, 2019, 571, 25-41.	2.2	61
97	Application of an Ion Beam Technique for the Design of Visible Light-Sensitive, Highly Efficient and Highly Selective Photocatalysts: Ion-Implantation and Ionized Cluster Beam Methods. Catalysis Surveys From Asia, 2004, 8, 35-45.	1.0	59
98	Ru nanoparticles confined in Zr-containing spherical mesoporous silica containers for hydrogenation of levulinic acid and its esters into Î <sup>3</sup> -valerolactone at ambient conditions. Catalysis Today, 2015, 258, 262-269.	2.2	59
99	Synthesis and Multifunctional Properties of Superparamagnetic Iron Oxide Nanoparticles Coated with Mesoporous Silica Involving Single-Site Tiâ^'Oxide Moiety. Journal of Physical Chemistry C, 2008, 112, 397-404.	1.5	57
100	Palladium Nanoparticles Supported on Titaniumâ€Doped Graphitic Carbon Nitride for Formic Acid Dehydrogenation. Chemistry - an Asian Journal, 2017, 12, 860-867.	1.7	57
101	Controlled release of hydrogen isotope compounds and tunneling effect in the heterogeneously-catalyzed formic acid dehydrogenation. Nature Communications, 2019, 10, 4094.	5.8	56
102	Characterization of the Local Structure of the Vanadium Silicalite (VS-2) Catalyst and Its Photocatalytic Reactivity for the Decomposition of NO into N2 and O2. Journal of Physical Chemistry B, 1999, 103, 9295-9301.	1.2	55
103	A novel synthetic route to hydroxyapatite–zeolite composite material from steel slag: investigation of synthesis mechanism and evaluation of physicochemical properties. Journal of Materials Chemistry, 2009, 19, 7263.	6.7	55
104	Synthesis and Unique Catalytic Performance of Single-Site Ti-Containing Hierarchical Macroporous Silica with Mesoporous Frameworks. Langmuir, 2011, 27, 2873-2879.	1.6	55
105	Direct observation of interfacial hole transfer from a photoexcited TiO2 particle to an adsorbed molecule SCN- by femtosecond diffuse reflectance spectroscopy. Research on Chemical Intermediates, 2001, 27, 177-187.	1.3	54
106	Photoinduced Aerobic Oxidation Driven by Phosphorescence Ir(III) Complex Anchored to Mesoporous Silica. Journal of Physical Chemistry C, 2011, 115, 21358-21362.	1.5	54
107	Ti cluster-alkylated hydrophobic MOFs for photocatalytic production of hydrogen peroxide in two-phase systems. Chemical Communications, 2019, 55, 6743-6746.	2.2	54
108	PdAg alloy nanoparticles encapsulated in N-doped microporous hollow carbon spheres for hydrogenation of CO2 to formate. Applied Catalysis B: Environmental, 2021, 283, 119628.	10.8	54

#	Article	IF	CITATIONS
109	Overcoming Acidic H <sub>2</sub> O <sub>2</sub> /Fe(II/III) Redox-Induced Low H <sub>2</sub> O <sub>2</sub> Utilization Efficiency by Carbon Quantum Dots Fenton-like Catalysis. Environmental Science & Technology, 2022, 56, 2617-2625.	4.6	54
110	Enhancement of Pd-catalyzed Suzuki–Miyaura coupling reaction assisted by localized surface plasmon resonance of Au nanorods. Catalysis Today, 2015, 242, 381-385.	2.2	53
111	Palladium Copper Chromium Ternary Nanoparticles Constructed Inâ€situ within a Basic Resin: Enhanced Activity in the Dehydrogenation of Formic Acid. ChemCatChem, 2017, 9, 3456-3462.	1.8	53
112	Applications of Single-site Photocatalysts to the Design of Unique Surface Functional Materials. Catalysis Surveys From Asia, 2008, 12, 88-100.	1.0	52
113	Silver Nanoparticles Supported on CeO <sub>2</sub> â€5BAâ€15 by Microwave Irradiation Possess Metal–Support Interactions and Enhanced Catalytic Activity. Chemistry - A European Journal, 2014, 20, 15746-15752.	1.7	52
114	Enhancement of Agâ€Based Plasmonic Photocatalysis in Hydrogen Production from Ammonia Borane by the Assistance of Singleâ€Site Tiâ€Oxide Moieties within a Silica Framework. Chemistry - A European Journal, 2017, 23, 3616-3622.	1.7	51
115	Hollow Mesoporous Organosilica Spheres Encapsulating PdAg Nanoparticles and Poly(Ethyleneimine) as Reusable Catalysts for CO <sub>2</sub> Hydrogenation to Formate. ACS Catalysis, 2020, 10, 6356-6366.	5.5	51
116	Recent Progress on Black Phosphorusâ€Based Materials for Photocatalytic Water Splitting. Small Methods, 2018, 2, 1800212.	4.6	50
117	Synthesis, characterization and photocatalytic reactivities of Mo-MCM-41 mesoporous molecular sieves: Effect of the Mo content on the local structures of Mo-oxides. Journal of Catalysis, 2005, 235, 272-278.	3.1	49
118	Synthesis of highly visible light active TiO <sub>2</sub> -2-naphthol surface complex and its application in photocatalytic chromium( <scp>vi</scp> ) reduction. RSC Advances, 2015, 5, 39752-39759.	1.7	49
119	Design of Singleâ€Site Photocatalysts by Using Metal–Organic Frameworks as a Matrix. Chemistry - an Asian Journal, 2018, 13, 1767-1779.	1.7	49
120	TiO2 photocatalyst loaded on hydrophobic Si3N4 support for efficient degradation of organics diluted in water. Applied Catalysis A: General, 2008, 350, 164-168.	2.2	48
121	One-pot synthesis of molybdenum oxide nanoparticles encapsulated in hollow silica spheres: an efficient and reusable catalyst for epoxidation of olefins. Journal of Materials Chemistry A, 2017, 5, 18518-18526.	5.2	48
122	Highly Dispersed Platinum Nanoparticles on TiO <sub>2</sub> Prepared by Using the Microwaveâ€Assisted Deposition Method: An Efficient Photocatalyst for the Formation of H <sub>2</sub> and N <sub>2</sub> from Aqueous NH <sub>3</sub> . Chemistry - an Asian Journal, 2012, 7, 1366-1371.	1.7	47
123	Poly(ethyleneimine)â€ŧethered Ir Complex Catalyst Immobilized in Titanate Nanotubes for Hydrogenation of CO <sub>2</sub> to Formic Acid. ChemCatChem, 2017, 9, 1906-1914.	1.8	47
124	Plasmonic metal/Mo <sub>x</sub> W <sub>1â^'x</sub> O <sub>3â^'y</sub> for visible-light-enhanced H <sub>2</sub> production from ammonia borane. Journal of Materials Chemistry A, 2018, 6, 10932-10938.	5.2	47
125	Enhanced simultaneous PEC eradication of bacteria and antibiotics by facilely fabricated high-activity {001} facets TiO2 mounted onto TiO2 nanotubular photoanode. Water Research, 2016, 101, 597-605.	5.3	46
126	Enhanced formic acid dehydrogenation by the synergistic alloying effect of PdCo catalysts supported on graphitic carbon nitride. International Journal of Hydrogen Energy, 2019, 44, 28483-28493.	3.8	46

#	Article	IF	CITATIONS
127	Dual Active Centers Bridged by Oxygen Vacancies of Ruthenium Singleâ€Atom Hybrids Supported on Molybdenum Oxide for Photocatalytic Ammonia Synthesis. Angewandte Chemie - International Edition, 2022, 61, .	7.2	45
128	Synthesis of zeolite from steel slag and its application as a support of nano-sized TiO2 photocatalyst. Journal of Materials Science, 2008, 43, 2407-2410.	1.7	44
129	Investigation of Size Sensitivity in the Hydrogen Production from Formic Acid over Carbonâ€Supported Pd Nanoparticles. ChemistrySelect, 2016, 1, 1879-1886.	0.7	44
130	Fabrication of Photocatalytic Paper Using TiO <sub>2</sub> Nanoparticles Confined in Hollow Silica Capsules. Langmuir, 2017, 33, 288-295.	1.6	44
131	Some novel porous materials for selective catalytic oxidations. Materials Today, 2020, 32, 244-259.	8.3	44
132	Active Site Design in a Core–Shell Nanostructured Catalyst for a Oneâ€Pot Oxidation Reaction. Chemistry - A European Journal, 2011, 17, 9047-9051.	1.7	43
133	Enhanced hydrogenation activity of nano-sized Pd–Ni bimetal particles on Ti-containing mesoporous silica prepared by a photo-assisted deposition method. Journal of Materials Chemistry, 2012, 22, 16243.	6.7	43
134	PdAg Nanoparticles within Core-Shell Structured Zeolitic Imidazolate Framework as a Dual Catalyst for Formic Acid-based Hydrogen Storage/Production. Scientific Reports, 2019, 9, 15675.	1.6	43
135	Metal–organic framework-based nanomaterials for photocatalytic hydrogen peroxide production. Physical Chemistry Chemical Physics, 2020, 22, 14404-14414.	1.3	43
136	In Situ Investigation of the Photocatalytic Decomposition of NO on the Tiâ^'HMS under Flow and Closed Reaction Systems. Journal of Physical Chemistry B, 2000, 104, 11501-11505.	1.2	42
137	Intercalation of Pt(II) Terpyridine Complexes into Layered K <sub>4</sub> Nb <sub>6</sub> O <sub>17</sub> and Visible-Light-Driven Photocatalytic Production of H <sub>2</sub> . Journal of Physical Chemistry C, 2012, 116, 18873-18877.	1.5	42
138	Hybrid Mesoporousâ€Silica Materials Functionalized by Pt <sup>II</sup> Complexes: Correlation between the Spatial Distribution of the Active Center, Photoluminescence Emission, and Photocatalytic Activity. Chemistry - A European Journal, 2012, 18, 11371-11378.	1.7	42
139	Metal Complexes Supported on Solid Matrices for Visibleâ€Lightâ€Driven Molecular Transformations. Chemistry - A European Journal, 2016, 22, 11122-11137.	1.7	42
140	Influence of Exchanged Alkali Metal Cations within Zeolite Y Cages on Spectroscopic and Photooxidation Properties of the Incorporated Tris(2,2′-bipyridine)ruthenium(II) Complexes. Journal of Physical Chemistry C, 2008, 112, 19449-19455.	1.5	41
141	Plasmonic Ru/hydrogen molybdenum bronzes with tunable oxygen vacancies for light-driven reduction of <i>p</i> -nitrophenol. Journal of Materials Chemistry A, 2019, 7, 3783-3789.	5.2	41
142	Construction of Hybrid MoS <sub>2</sub> Phase Coupled with SiC Heterojunctions with Promoted Photocatalytic Activity for 4-Nitrophenol Degradation. Langmuir, 2020, 36, 1174-1182.	1.6	41
143	Anchoring of Pt(II) Pyridyl Complex to Mesoporous Silica Materials: Enhanced Photoluminescence Emission at Room Temperature and Photooxidation Activity using Molecular Oxygen. Journal of Physical Chemistry C, 2011, 115, 1044-1050.	1.5	40
144	Insights on palladium decorated nitrogen-doped carbon xerogels for the hydrogen production from formic acid. Catalysis Today, 2019, 324, 90-96.	2.2	40

#	Article	IF	CITATIONS
145	Lipase-embedded silica nanoparticles with oil-filled core–shell structure: stable and recyclable platforms for biocatalysts. Chemical Communications, 2012, 48, 2882.	2.2	39
146	Structural Design of Pd/SiO <sub>2</sub> @Ti-Containing Mesoporous Silica Core–Shell Catalyst for Efficient One-Pot Oxidation Using in Situ Produced H <sub>2</sub> O <sub>2</sub> . Journal of Physical Chemistry C, 2012, 116, 14360-14367.	1.5	39
147	Pd/zeolite-based catalysts for the preferential CO oxidation reaction: ion-exchange, Si/Al and structure effect. Catalysis Science and Technology, 2016, 6, 2623-2632.	2.1	39
148	Multifunctional surface designed by nanocomposite coating of polytetrafluoroethylene and TiO2 photocatalyst: self-cleaning and superhydrophobicity. Scientific Reports, 2017, 7, 13628.	1.6	39
149	Defect Engineering of MoS <sub>2</sub> and Its Impacts on Electrocatalytic and Photocatalytic Behavior in Hydrogen Evolution Reactions. Chemistry - an Asian Journal, 2019, 14, 278-285.	1.7	39
150	PdAg nanoparticles supported on resorcinol-formaldehyde polymers containing amine groups: the promotional effect of phenylamine moieties on CO <sub>2</sub> transformation to formic acid. Journal of Materials Chemistry A, 2019, 7, 16356-16363.	5.2	39
151	Introduction of a secondary ligand into titanium-based metal–organic frameworks for visible-light-driven photocatalytic hydrogen peroxide production from dioxygen reduction. Journal of Materials Chemistry A, 2021, 9, 2815-2821.	5.2	39
152	Revealing hydrogen spillover pathways in reducible metal oxides. Chemical Science, 2022, 13, 8137-8147.	3.7	39
153	Size-controlled synthesis of silver nanoparticles on Ti-containing mesoporous silica thin film and photoluminescence enhancement of rhodamine 6G dyes by surface plasmon resonance. Journal of Materials Chemistry, 2009, 19, 6745.	6.7	38
154	Liquid-phase oxidation of alkylaromatics to aromatic ketones with molecular oxygen over a Mn-based metal–organic framework. Dalton Transactions, 2017, 46, 8415-8421.	1.6	38
155	Visible-light-driven hydrogen peroxide production from water and dioxygen by perylenetetracarboxylic diimide modified titanium-based metal–organic frameworks. Journal of Materials Chemistry A, 2021, 9, 26371-26380.	5.2	38
156	Synthesis and Characterization of Coreâ^'Shell FePt@Ti-Containing Silica Spherical Nanocomposite as a Catalyst Carrier for Liquid-Phase Reactions. Journal of Physical Chemistry C, 2008, 112, 16478-16483.	1.5	37
157	Controlled synthesis of carbon-supported Co catalysts from single-sites to nanoparticles: characterization of the structural transformation and investigation of their oxidation catalysis. Physical Chemistry Chemical Physics, 2017, 19, 4967-4974.	1.3	37
158	CoO <sub>x</sub> -decorated CeO <sub>2</sub> heterostructures: effects of morphology on their catalytic properties in diesel soot combustion. Nanoscale, 2020, 12, 1779-1789.	2.8	37
159	Synthesis of mesoporous silica-supported Ag nanorod-based bimetallic catalysts and investigation of their plasmonic activity under visible light irradiation. Catalysis Science and Technology, 2017, 7, 2551-2558.	2.1	36
160	Photocatalytic decomposition of NO on Ti-HMS mesoporous zeolite catalysts. Catalysis Letters, 2000, 66, 241-243.	1.4	35
161	Screening of Carbon-Supported PdAg Nanoparticles in the Hydrogen Production from Formic Acid. Industrial & Engineering Chemistry Research, 2016, 55, 7612-7620.	1.8	35
162	Synthesis of carbon-supported Pd–Co bimetallic catalysts templated by Co nanoparticles using the galvanic replacement method for selective hydrogenation. RSC Advances, 2017, 7, 22294-22300.	1.7	35

#	Article	IF	CITATIONS
163	Plasmonic catalysis of Ag nanoparticles deposited on CeO2 modified mesoporous silica for the nitrostyrene reduction under light irradiation conditions. Catalysis Today, 2019, 324, 83-89.	2.2	35
164	A quasi-stable molybdenum sub-oxide with abundant oxygen vacancies that promotes CO <sub>2</sub> hydrogenation to methanol. Chemical Science, 2021, 12, 9902-9915.	3.7	35
165	Photoluminescence Emission and Photoinduced Hydrogen Production Driven by Pt <sup>II</sup> Pyridyl Complexes Anchored onto Mesoporous Silica. Chemistry - A European Journal, 2012, 18, 415-418.	1.7	34
166	Effect of the Si/Al Ratio on the Local Structure of V Oxide/ZSM-5 Catalysts Prepared by Solid-State Reaction and Their Photocatalytic Reactivity for the Decomposition of NO in the Absence and Presence of Propane. Journal of Physical Chemistry B, 2000, 104, 10288-10292.	1.2	33
167	Preparation of Unique TiO2 Nano-particle Photocatalysts by a Multi-gelation Method for Control of the Physicochemical Parameters and Reactivity. Catalysis Letters, 2005, 105, 111-117.	1.4	33
168	Synthesis of a Fe–Ni Alloy on a Ceria Support as a Nobleâ€Metalâ€Free Catalyst for Hydrogen Production from Chemical Hydrogen Storage Materials. ChemCatChem, 2015, 7, 1285-1291.	1.8	33
169	Roomâ€Temperature and Aqueousâ€Phase Synthesis of Plasmonic Molybdenum Oxide Nanoparticles for Visibleâ€Lightâ€Enhanced Hydrogen Generation. Chemistry - an Asian Journal, 2016, 11, 2377-2381.	1.7	33
170	Engineering of Surface Environment of Pd Nanoparticle Catalysts on Carbon Support with Pyrene–Thiol Ligands for Semihydrogenation of Alkynes. ACS Applied Materials & Interfaces, 2019, 11, 37708-37719.	4.0	33
171	Design of mesoporous silica thin films containing single-site photocatalysts and their applications to superhydrophilic materials. Applied Catalysis A: General, 2011, 400, 1-8.	2.2	32
172	Wasteâ€Slag Hydrocalumite and Derivatives as Heterogeneous Base Catalysts. ChemSusChem, 2012, 5, 1523-1532.	3.6	32
173	Microwave-antenna induced in situ synthesis of Cu nanowire threaded ZIF-8 with enhanced catalytic activity in H <sub>2</sub> production. Nanoscale, 2016, 8, 7749-7754.	2.8	32
174	Synthesis of plasmonic gold nanoparticles supported on morphology-controlled TiO2 for aerobic alcohol oxidation. Catalysis Today, 2020, 352, 255-261.	2.2	32
175	Synthesis of a binary alloy nanoparticle catalyst with an immiscible combination of Rh and Cu assisted by hydrogen spillover on a TiO <sub>2</sub> support. Chemical Science, 2020, 11, 4194-4203.	3.7	32
176	An Efficient Cu/BaO/La <sub>2</sub> O <sub>3</sub> Catalyst for the Simultaneous Removal of Carbon Soot and Nitrogen Oxides from Simulated Diesel Exhaust. Journal of Physical Chemistry C, 2014, 118, 9078-9085.	1.5	31
177	Catalytic combustion of diesel soot over Fe and Ag-doped manganese oxides: role of heteroatoms in the catalytic performances. Catalysis Science and Technology, 2018, 8, 1905-1914.	2.1	31
178	Design of Pd–Graphene–Au Nanorod Nanocomposite Catalyst for Boosting Suzuki–Miyaura Coupling Reaction by Assistance of Surface Plasmon Resonance. Journal of Physical Chemistry C, 2019, 123, 24575-24583.	1.5	31
179	Incorporation of a Ru complex into an amine-functionalized metal–organic framework for enhanced activity in photocatalytic aerobic benzyl alcohol oxidation. Catalysis Science and Technology, 2019, 9, 1511-1517.	2.1	31
180	Design of Silver-Based Controlled Nanostructures for Plasmonic Catalysis under Visible Light Irradiation. Bulletin of the Chemical Society of Japan, 2019, 92, 19-29.	2.0	31

#	Article	IF	CITATIONS
181	Plasmon-induced catalytic CO <sub>2</sub> hydrogenation by a nano-sheet Pt/H <sub>x</sub> MoO <sub>3â^'y</sub> hybrid with abundant surface oxygen vacancies. Journal of Materials Chemistry A, 2021, 9, 13898-13907.	5.2	31
182	PdAg nanoparticles and aminopolymer confined within mesoporous hollow carbon spheres as an efficient catalyst for hydrogenation of CO <sub>2</sub> to formate. Journal of Materials Chemistry A, 2020, 8, 4437-4446.	5.2	31
183	Electrochemical Reactors for Continuous Decentralized H <sub>2</sub> O <sub>2</sub> Production. Angewandte Chemie - International Edition, 2022, 61, .	7.2	31
184	State of Pt in Dried and Reduced PtIn and PtSn Catalysts Supported on Carbon. Journal of Physical Chemistry C, 2007, 111, 4710-4716.	1.5	30
185	Oxidation of Benzyl Alcohol over Nanoporous Au–CeO <sub>2</sub> Catalysts Prepared from Amorphous Alloys and Effect of Alloying Au with Amorphous Alloys. Industrial & Engineering Chemistry Research, 2018, 57, 5599-5605.	1.8	30
186	Twoâ€Phase System Utilizing Hydrophobic Metal–Organic Frameworks (MOFs) for Photocatalytic Synthesis of Hydrogen Peroxide. Angewandte Chemie, 2019, 131, 5456-5460.	1.6	30
187	Visible-light driven H2 production utilizing iridium and rhodium complexes intercalated into a zirconium phosphate layered matrix. Dalton Transactions, 2014, 43, 10541.	1.6	29
188	Facile Synthesis of Yolk–Shell Nanostructured Photocatalyst with Improved Adsorption Properties and Molecular‣ieving Properties. ChemCatChem, 2016, 8, 2781-2788.	1.8	29
189	Visible-light-enhanced catalytic activity of Ru nanoparticles over carbon modified g-C3N4. Journal of Photochemistry and Photobiology A: Chemistry, 2018, 358, 327-333.	2.0	29
190	New insight on electroreduction of nitrate to ammonia driven by oxygen vacancies-induced strong interface interactions. Journal of Catalysis, 2022, 406, 39-47.	3.1	29
191	Visible-light-responsive photocatalytic reaction on tetrahedrally-coordinated chromium oxide moieties loaded on ZSM-5 zeolites and HMS mesoporous silica: partial oxidation of propane. Research on Chemical Intermediates, 2003, 29, 881-890.	1.3	28
192	Photo-induced super-hydrophilic property and photocatalysis on transparent Ti-containing mesoporous silica thin films. Catalysis Today, 2006, 111, 254-258.	2.2	28
193	In Situ Generation of Active Pd Nanoparticles within a Macroreticular Acidic Resin: Efficient Catalyst for the Direct Synthesis of Hydrogen Peroxide. Journal of Physical Chemistry Letters, 2010, 1, 1675-1678.	2.1	28
194	Nickel-supported carbon nitride photocatalyst combined with organic dye for visible-light-driven hydrogen evolution from water. Physical Chemistry Chemical Physics, 2015, 17, 24086-24091.	1.3	28
195	How the Morphology of NiO <i><sub>x</sub></i> -Decorated CeO <sub>2</sub> Nanostructures Affects Catalytic Properties in CO <sub>2</sub> Methanation. Langmuir, 2021, 37, 5376-5384.	1.6	28
196	Photocatalytic performance of TiO <sub>2</sub> –zeolite templated carbon composites in organic contaminant degradation. Physical Chemistry Chemical Physics, 2014, 16, 25004-25007.	1.3	27
197	Interconversion of Formate/Bicarbonate for Hydrogen Storage/Release: Improved Activity Following Sacrificial Surface Modification of a Ag@Pd/TiO <sub>2</sub> Catalyst with a TiO <i><sub>x</sub></i> Shell. ACS Applied Energy Materials, 2020, 3, 5819-5829.	2.5	27
198	Recent strategies for enhancing the catalytic activity of CO2 hydrogenation to formate/formic acid over Pd-based catalyst. Journal of CO2 Utilization, 2021, 54, 101765.	3.3	27

#	Article	IF	CITATIONS
199	Dual Role of Missing-Linker Defects Terminated by Acetate Ligands in a Zirconium-Based MOF in Promoting Photocatalytic Hydrogen Peroxide Production. Journal of Physical Chemistry C, 2021, 125, 27909-27918.	1.5	27
200	Ru/H MoO3- with plasmonic effect for boosting photothermal catalytic CO2 methanation. Applied Catalysis B: Environmental, 2022, 317, 121734.	10.8	27
201	Size Effect of Carbon-Supported Pd Nanoparticles in the Hydrogen Production from Formic Acid. Bulletin of the Chemical Society of Japan, 2015, 88, 1500-1502.	2.0	26
202	Visibleâ€Lightâ€Responsive Carbon Dioxide Reduction System: Rhenium Complex Intercalated into a Zirconium Phosphate Layered Matrix. ChemCatChem, 2015, 7, 3519-3525.	1.8	26
203	Simple Route for the Synthesis of Highly Active Bimetallic Nanoparticle Catalysts with Immiscible Ru and Ni Combination by utilizing a TiO <sub>2</sub> Support. ChemCatChem, 2018, 10, 3526-3531.	1.8	26
204	Supported Pd and PdAu Nanoparticles on Ti-MCM-41 Prepared by a Photo-assisted Deposition Method as Efficient Catalysts for Direct Synthesis of H2O2 from H2 and O2. Catalysis Letters, 2009, 131, 337-343.	1.4	25
205	Pd–Cu Alloy Nanoparticles Confined within Mesoporous Hollow Carbon Spheres for the Hydrogenation of CO <sub>2</sub> to Formate. Journal of Physical Chemistry C, 2021, 125, 3961-3971.	1.5	25
206	Title is missing!. Catalysis Letters, 2000, 68, 101-103.	1.4	24
207	Heterometallic and Hydrophobic Metal–Organic Frameworks as Durable Photocatalysts for Boosting Hydrogen Peroxide Production in a Two-Phase System. ACS Applied Energy Materials, 2021, 4, 4823-4830.	2.5	24
208	Preparation of Superhydrophilic Mesoporous Silica Thin Films Containing Single-site Photocatalyst (Ti, V, Cr, Mo, and W oxide moieties). Chemistry Letters, 2008, 37, 748-749.	0.7	23
209	An electroless deposition technique for the synthesis of highly active and nano-sized Pd particles on silica nanosphere. Catalysis Today, 2012, 185, 109-112.	2.2	23
210	Activity, Recyclability, and Stability of Lipases Immobilized on Oilâ€Filled Spherical Silica Nanoparticles with Different Silica Shell Structures. ChemCatChem, 2013, 5, 2527-2536.	1.8	23
211	Preparation of single-site Ti-containing mesoporous silica with a nanotube architecture and its enhanced catalytic activities. Journal of Materials Chemistry A, 2013, 1, 891-897.	5.2	23
212	Creation of Nickel-Based Active Species within a Macroreticular Acidic Resin: A Noble-Metal-Free Heterogeneous Catalyst for Visible-Light-Driven H <sub>2</sub> Evolution from Water. ACS Catalysis, 2014, 4, 4129-4135.	5.5	23
213	Design of Composite Photocatalyst of TiO2 and Y-Zeolite for Degradation of 2-Propanol in the Gas Phase under UV and Visible Light Irradiation. Molecules, 2014, 19, 16477-16488.	1.7	23
214	Phosphate Removal from Aqueous Solutions Using Calcium Silicate Hydrate Prepared from Blast Furnace Slag. ISIJ International, 2017, 57, 1657-1664.	0.6	23
215	Tailoring the Size and Shape of Colloidal Noble Metal Nanocrystals as a Valuable Tool in Catalysis. Catalysis Surveys From Asia, 2019, 23, 127-148.	1.0	23
216	Photoluminescence properties of tetrahedral titanium oxide species in zeolitic materials. Catalysis Letters, 1998, 53, 107-109.	1.4	22

#	Article	IF	CITATIONS
217	Synthesize of nano-sized Pd metal catalyst on Ti-containing zeolite using a photo-assisted deposition (PAD) method. Catalysis Letters, 2007, 114, 75-78.	1.4	22
218	Preparation of hydrophobically modified single-site Ti-containing mesoporous silica (TiSBA-15) and their enhanced catalytic performances. Catalysis Today, 2011, 175, 393-397.	2.2	22
219	Elaboration, characterization and properties of silica-based single-site heterogeneous photocatalysts. Proceedings of the Royal Society A: Mathematical, Physical and Engineering Sciences, 2012, 468, 2113-2128.	1.0	22
220	Enhancement of Catalytic Activity Over AuPd Nanoparticles Loaded Metal Organic Framework Under Visible Light Irradiation. Topics in Catalysis, 2016, 59, 1765-1771.	1.3	22
221	Removal of Phosphate from Aqueous Solution Using Layered Double Hydroxide Prepared from Waste Iron-Making Slag. Bulletin of the Chemical Society of Japan, 2016, 89, 472-480.	2.0	22
222	In situ-created Mn( <scp>iii</scp> ) complexes active for liquid-phase oxidation of alkylaromatics to aromatic ketones with molecular oxygen. Catalysis Science and Technology, 2016, 6, 442-448.	2.1	22
223	Interfacial Engineering of PdAg/TiO <sub>2</sub> with a Metal–Organic Framework to Promote the Hydrogenation of CO <sub>2</sub> to Formic Acid. Journal of Physical Chemistry C, 2020, 124, 11499-11505.	1.5	22
224	Additive-Free Aqueous Phase Synthesis of Formic Acid by Direct CO2 Hydrogenation over a PdAg Catalyst on a Hydrophilic N-Doped Polymer–Silica Composite Support with High CO2 Affinity. ACS Applied Energy Materials, 2020, 3, 5847-5855.	2.5	22
225	Plasmonic nanocatalysts for visible-NIR light induced hydrogen generation from storage materials. Materials Advances, 2021, 2, 880-906.	2.6	22
226	Frontiers of Photo-catalysis and Photo-reaction at Solid Surfaces. Design and Development of a Titanium Oxide Photocatalyst Able to Work Effectively under Visible Light Irradiation by an Advanced Metal Ion-Implantation Method Hyomen Kagaku, 1999, 20, 60-65.	0.0	22
227	Investigation of local structures and photo-induced surface properties on transparent Me(Ti,Cr)-containing mesoporous silica thin films. Microporous and Mesoporous Materials, 2007, 101, 288-295.	2.2	21
228	Low-temperature synthesis of highly hydrophilic Ti-containing mesoporous silica thin films on polymer substrates by photocatalytic removal of structure-directing agents. Journal of Materials Chemistry, 2011, 21, 236-241.	6.7	21
229	Palladium Nanoparticles Encapsulated in Hollow Titanosilicate Spheres as an Ideal Nanoreactor for Oneâ€pot Oxidation. Chemistry - A European Journal, 2017, 23, 380-389.	1.7	21
230	Ultra‣ow Loading of Ru Clusters over Graphitic Carbon Nitride: A Drastic Enhancement in Photocatalytic Hydrogen Evolution Activity. ChemCatChem, 2019, 11, 1963-1969.	1.8	21
231	Design and application of photocatalysts using porous materials. Catalysis Reviews - Science and Engineering, 2021, 63, 165-233.	5.7	21
232	Defect Engineering of Pt/TiO <sub>2–<i>x</i></sub> Photocatalysts via Reduction Treatment Assisted by Hydrogen Spillover. ACS Applied Materials & Interfaces, 2021, 13, 48669-48678.	4.0	21
233	Design of Single-Site Ti Embedded Highly Hydrophilic Silica Thin Films with Macro–Mesoporous Structures. ACS Applied Materials & Interfaces, 2011, 3, 4561-4565.	4.0	20
234	Synthesis of Pd nanoparticles on heteropolyacid-supported silica by a photo-assisted deposition method: an active catalyst for the direct synthesis of hydrogen peroxide. RSC Advances, 2012, 2, 1047-1054.	1.7	20

#	Article	IF	CITATIONS
235	Environmental Transmission Electron Microscopy Study of Diesel Carbon Soot Combustion under Simulated Catalyticâ€Reaction Conditions. ChemPhysChem, 2015, 16, 1347-1351.	1.0	20
236	Shape Effect of MnO <i>x</i> -Decorated CeO2 Catalyst in Diesel Soot Oxidation. Bulletin of the Chemical Society of Japan, 2017, 90, 556-564.	2.0	20
237	Synthesis of Nano-Sized Platinum Metal Particles on Ti-Containing Mesoporous Silica Using Microwave-Assisted Deposition Method. Topics in Catalysis, 2010, 53, 218-223.	1.3	19
238	Iridium and Rhodium Complexes within a Macroreticular Acidic Resin: A Heterogeneous Photocatalyst for Visibleâ€ŀight Driven H <sub>2</sub> Production without an Electron Mediator. Chemistry - an Asian Journal, 2013, 8, 3207-3213.	1.7	19
239	Hollow titanosilicate nanospheres encapsulating PdAu alloy nanoparticles as reusable high-performance catalysts for a H <sub>2</sub> O <sub>2</sub> -mediated one-pot oxidation reaction. Journal of Materials Chemistry A, 2019, 7, 7221-7231.	5.2	19
240	Luminescent Single-Atom Eu-Coordinated Graphitic Carbon Nitride Nanosheets for Selective Sensing of Acetone and Cyclohexane. ACS Applied Nano Materials, 2020, 3, 10209-10217.	2.4	19
241	Photocatalytically-driven H2 production over Cu/TiO2 catalysts decorated with multi-walled carbon nanotubes. Catalysis Today, 2021, 364, 182-189.	2.2	19
242	An efficient method for the creation of a superhydrophobic surface: ethylene polymerization over self-assembled colloidal silica nanoparticles incorporating single-site Cr-oxide catalysts. Journal of Materials Chemistry, 2011, 21, 8543.	6.7	18
243	Reactivity of Ni–Carbon Nanofibers/Mesocellular Silica Composite Catalyst for Phenylacetylene Hydrogenation. Industrial & Engineering Chemistry Research, 2014, 53, 10105-10111.	1.8	18
244	A direct conversion of blast furnace slag to a mesoporous silica–calcium oxide composite and its application in CO <sub>2</sub> captures. Green Chemistry, 2020, 22, 3759-3768.	4.6	18
245	Photocatalytic decomposition of N2O on Cu+/Y-zeolite catalysts prepared by ion-exchange. Korean Journal of Chemical Engineering, 1997, 14, 498-501.	1.2	17
246	Photocatalytic epoxidation of propene with molecular oxygen under visible light irradiation on V ion-implanted Ti-HMS and Cr-HMS mesoporous molecular sieves. Studies in Surface Science and Catalysis, 2003, 146, 597-600.	1.5	17
247	A new application of photocatalysts: synthesis of nano-sized metal and alloy catalysts by a photo-assisted deposition method. Photochemical and Photobiological Sciences, 2009, 8, 652-656.	1.6	17
248	Controlled Synthesis and Surface Hydrophilic Properties of Ti-Containing Mesoporous Silica Thin Films Using Various Structure-Directing Agents. Journal of Physical Chemistry C, 2011, 115, 15410-15415.	1.5	17
249	Control of physicochemical properties and catalytic activity of tris(2,2′-bipyridine)iron( <scp>ii</scp> ) encapsulated within the zeolite Y cavity by alkaline earth metal cations. Dalton Transactions, 2014, 43, 1132-1138.	1.6	17
250	Controlling Photocatalytic Activity and Size Selectivity of TiO <sub>2</sub> Encapsulated in Hollow Silica Spheres by Tuning Silica Shell Structures Using Sacrificial Biomolecules. Langmuir, 2017, 33, 6314-6321.	1.6	17
251	Photocatalytic properties of TiO2-loaded porous silica with hierarchical macroporous and mesoporous architectures in the degradation of gaseous organic molecules. Catalysis Today, 2019, 332, 222-226.	2.2	17
252	Photocatalytic Approaches for Hydrogen Production via Formic Acid Decomposition. Topics in Current Chemistry, 2019, 377, 27.	3.0	17

#	Article	IF	CITATIONS
253	Photocatalytic Reduction of CO <sub>2</sub> with H <sub>2</sub> O on Titanium Oxides Prepared within Zeolites and Mesoporous Molecular Sieves. Electrochemistry, 2002, 70, 402-408.	0.6	16
254	Catalysis of nanosized Pd metal catalyst deposited on Ti-containing zeolite by a photo-assisted deposition (PAD) method. Pure and Applied Chemistry, 2007, 79, 2095-2100.	0.9	16
255	Application of Microwave-Assisted Deposition for the Synthesis of Noble Metal Particles on Ti-Containing Mesoporous Silica. Catalysis Letters, 2009, 129, 404-407.	1.4	16
256	Mesoporous silica supported Pd/Ag bimetallic nanoparticles as a plasmonic catalyst for chemoselective hydrogenation of p-nitrostyrene under visible light irradiation. Journal of Chemical Sciences, 2017, 129, 1661-1669.	0.7	16
257	Crystal Facet Engineering and Hydrogen Spillover-Assisted Synthesis of Defective Pt/TiO <sub>2–<i>x</i></sub> Nanorods with Enhanced Visible Light-Driven Photocatalytic Activity. ACS Applied Materials & Interfaces, 2022, 14, 2291-2300.	4.0	16
258	Enhanced visible-NIR absorption and oxygen vacancy generation of Pt/H <sub><i>x</i></sub> MoWO <sub><i>y</i></sub> by H-spillover to facilitate photothermal catalytic CO <sub>2</sub> hydrogenation. Journal of Materials Chemistry A, 2022, 10, 10854-10864.	5.2	16
259	Surface hydrophilic–hydrophobic property on transparent mesoporous silica thin films containing chromium oxide single-site photocatalyst. Catalysis Today, 2008, 132, 146-152.	2.2	15
260	Fabrication of Hydrophobic Zeolites Using Triethoxyfluorosilane and their Application for Photocatalytic Degradation of Acetaldehyde. Topics in Catalysis, 2009, 52, 643-648.	1.3	15
261	Preparation of Cr–Ti Binary Oxide Anchored Mesoporous Silica by CVD Method and Their Photocatalytic Activities. Topics in Catalysis, 2010, 53, 555-559.	1.3	15
262	Design of superhydrophobic surfaces by synthesis of carbon nanotubes over Co–Mo nanocatalysts deposited under microwave irradiation on Ti-containing mesoporous silica thin films. Physical Chemistry Chemical Physics, 2011, 13, 6309.	1.3	15
263	ã,³āƒā,╋ƒ‰çжãŠã,ˆã³æ‹…æŒãƒŠãƒŽç²'åã®è¨è¨ˆâ"€ãã®åªæˆ¥¼Œæ§‹é€è§£æžãë触媒作用─. Journal of tl	ne <b>jap</b> an P	etr <del>p</del> leum Insti
264	Skeletal Ni Catalysts Prepared from Amorphous Ni–Zr Alloys: Enhanced Catalytic Performance for Hydrogen Generation from Ammonia Borane. ChemPhysChem, 2016, 17, 412-417.	1.0	15
265	Properties, fabrication and applications of plasmonic semiconductor nanocrystals. Catalysis Science and Technology, 2020, 10, 4141-4163.	2.1	15
266	Recent Applications of Amorphous Alloys to Design Skeletal Catalysts. Bulletin of the Chemical Society of Japan, 2020, 93, 438-454.	2.0	15
267	Characterization of Ti/Si binary oxides prepared by the sol-gel method and their photocatalytic properties: The hydrogenation and hydrogenolysis of CH3CCH with H2O. Korean Journal of Chemical Engineering, 1998, 15, 491-495.	1.2	14
268	Preparation of highly active platinum nanoparticles on ZSM-5 zeolite including cerium and titanium dioxides as photo-assisted deposition sites. Catalysis Today, 2010, 153, 189-192.	2.2	14
269	Effect of alkaline-earth species in phosphate glasses on the mobility of proton carriers. Journal of Materials Chemistry A, 2017, 5, 12385-12392.	5.2	14
270	Black Phosphorusâ€Based Compound with Few Layers for Photocatalytic Water Oxidation. ChemCatChem, 2018, 10, 3424-3428.	1.8	14

#	Article	IF	CITATIONS
271	Visible-light-driven reduction of nitrostyrene utilizing plasmonic silver nanoparticle catalysts immobilized on oxide supports. Catalysis Today, 2020, 355, 620-626.	2.2	14
272	Direct Synthesis of a Regenerative CaO–Fe <sub>3</sub> O <sub>4</sub> –SiO <sub>2</sub> Composite Adsorbent from Converter Slag for CO <sub>2</sub> Capture Applications. ACS Sustainable Chemistry and Engineering, 2022, 10, 372-381.	3.2	14
273	Photocatalytic Reduction of CO2with H2O on Various Titanium Oxide Catalysts. ACS Symposium Series, 2002, , 330-343.	0.5	13
274	Design of superhydrophilic surfaces on metallic substrates by the fabrication of Ti-containing mesoporous silica thin film. Applied Catalysis A: General, 2010, 387, 95-99.	2.2	13
275	Preparation of aluminum-containing mesoporous silica with hierarchical macroporous architecture and its enhanced catalytic activities. Physical Chemistry Chemical Physics, 2013, 15, 13323.	1.3	13
276	Enhanced ammonia-borane decomposition by synergistic catalysis using CoPd nanoparticles supported on titano-silicates. RSC Advances, 2016, 6, 91768-91772.	1.7	13
277	Improvement of the water oxidation performance of Ti, F co-modified hematite by surface modification with a Co(salen) molecular cocatalyst. Journal of Materials Chemistry A, 2020, 8, 21613-21622.	5.2	13
278	Photoreduction of Carbon Dioxide to Formic Acid with Fe-Based MOFs: The Promotional Effects of Heteroatom Doping and Alloy Nanoparticle Confinement. ACS Applied Energy Materials, 2021, 4, 11634-11642.	2.5	13
279	New insights in establishing the structure-property relations of novel plasmonic nanostructures for clean energy applications. EnergyChem, 2022, 4, 100070.	10.1	13
280	Photocatalytic Reduction of CO2 with H2O on Ti-Containing Mesoporous Silica Hydrophobically Modified Using Fluoride Ions. Studies in Surface Science and Catalysis, 2004, 153, 289-294.	1.5	12
281	Active Skeletal Ni Catalysts Prepared from an Amorphous Niâ€Zr Alloy in the Preâ€Crystallization State. ChemPhysChem, 2013, 14, 2534-2538.	1.0	12
282	Uniform anatase single-crystal cubes with high thermal stability fully enclosed by active {010} and {001} facets. RSC Advances, 2015, 5, 11029-11035.	1.7	12
283	Active skeletal Ni catalysts prepared from Ni–Zr amorphous alloys by oxygen treatment. Applied Catalysis A: General, 2015, 504, 559-564.	2.2	12
284	Skeletal Au prepared from Au–Zr amorphous alloys with controlled atomic compositions and arrangement for active oxidation of benzyl alcohol. Journal of Materials Chemistry A, 2016, 4, 8458-8465.	5.2	12
285	Self-assembled core–shell nanocomposite catalysts consisting of single-site Co-coordinated g-C3N4 and Au nanorods for plasmon-enhanced CO2 reduction. Journal of CO2 Utilization, 2021, 52, 101691.	3.3	12
286	Electrochemical Reactors for Continuous Decentralized H <sub>2</sub> O <sub>2</sub> Production. Angewandte Chemie, 2022, 134, .	1.6	12
287	Fluorescence Properties of 2,5-Bis(4-(diethylamino)phenyl)-1,3,4-oxadiazole Molecules Encapsulated in SiO2 and Siâ^'Ti Binary Oxide Matrixes by the Solâr'Gel Method. Langmuir, 1999, 15, 77-82.	1.6	11
288	Design of TiO 2 /Activated Carbon Fiber Systems by An Ionized Cluster Beam Method and Their Application for the Photocatalytic Water Purification. Molecular Crystals and Liquid Crystals, 2002, 388, 39-44.	0.4	11

#	Article	IF	CITATIONS
289	Photo-induced Surface Property on Transparent Mesoporous Silica Thin Films Containing Single-site Photocatalyst. Topics in Catalysis, 2008, 47, 116-121.	1.3	11
290	Synthesis and Characterization of Ir and Rh Complexes Supported on Layered K4Nb6O17 as a Heterogeneous Photocatalyst for Visible-Light-Induced Hydrogen Evolution. Bulletin of the Chemical Society of Japan, 2014, 87, 874-881.	2.0	11
291	Pyreneâ€Thiolâ€modified Pd Nanoparticles on Carbon Support: Kinetic Control by Steric Hinderance and Improved Stability by the Catalystâ€Support Interaction. ChemCatChem, 2020, 12, 5880-5887.	1.8	11
292	Promotional effect of surface plasmon resonance on direct formation of hydrogen peroxide from H2 and O2 over Pd/Graphene-Au nanorod catalytic system. Journal of Catalysis, 2021, 394, 259-265.	3.1	11
293	Synthesis of Highly Dispersed Platinum Nanoparticles on Ti-Containing Mesoporous Silica Using Photo-Assisted Deposition. Journal of Nanoscience and Nanotechnology, 2009, 9, 557-561.	0.9	10
294	Size-controlled deposition of Ag nanoparticles on alumina with the assistance of a photo-induced chromic reaction, and study of their catalytic properties. Physical Chemistry Chemical Physics, 2011, 13, 15821.	1.3	10
295	Preparation of Skeletal Cu Catalysts by Thermal and Chemical Treatment of Cu–Ti Amorphous Alloys and Their Enhanced Catalytic Activities. Bulletin of the Chemical Society of Japan, 2013, 86, 1002-1004.	2.0	10
296	Hydroxylation of Phenol on Iron-Containing Mesoporous Silica with Hierarchical Macroporous Architecture. Bulletin of the Chemical Society of Japan, 2015, 88, 572-574.	2.0	10
297	Ruthenium(II)â^'Bipyridine/NanoC <sub>3</sub> N <sub>4</sub> Hybrids: Tunable Photochemical Properties by Using Exchangeable Alkali Metal Cations. Chemistry - an Asian Journal, 2018, 13, 1348-1356.	1.7	10
298	RuPd Alloy Nanoparticles Supported on Plasmonic H x MoO3-y for Efficient Photocatalytic Reduction of p -Nitrophenol. European Journal of Inorganic Chemistry, 2019, 2019, 3745-3752.	1.0	10
299	Diesel Soot Combustion over Mn 2 O 3 Catalysts with Different Morphologies: Elucidating the Role of Active Oxygen Species in Soot Combustion. Chemistry - an Asian Journal, 2020, 15, 2005-2014.	1.7	10
300	Enhanced Catalysis of Plasmonic Silver Nanoparticles by a Combination of Macro-/Mesoporous Nanostructured Silica Support. Journal of Physical Chemistry C, 2021, 125, 9150-9157.	1.5	10
301	Morphology-controlled Pd nanocrystals as catalysts in tandem dehydrogenation-hydrogenation reactions. Journal of Chemical Sciences, 2017, 129, 1695-1703.	0.7	10
302	Preparation of Thin Macroporous TiO2 Films Using PMMA Microspheres and Their Photoinduced Hydrophilicities. Chemistry Letters, 2009, 38, 610-611.	0.7	9
303	Synthesis of Ag nanoparticles encapsulated in hollow silica spheres for efficient and selective removal of low-concentrated sulfur compounds. Journal of Materials Chemistry A, 2017, 5, 25431-25437.	5.2	9
304	Effects of Carbon Support Nanostructures on the Reactivity of a Ru Nanoparticle Catalyst in a Hydrogen Transfer Reaction. Organic Process Research and Development, 2018, 22, 1580-1585.	1.3	9
305	Modification of Tiâ€doped Hematite Photoanode with Quasiâ€molecular Cocatalyst: A Comparison of Improvement Mechanism Between Nonâ€noble and Noble Metals. ChemSusChem, 2021, 14, 2180-2187.	3.6	9
306	Synthesis of a CaO-Fe2O3-SiO2 composite from a dephosphorization slag for adsorption of CO2. Catalysis Today, 2023, 410, 264-272.	2.2	9

#	Article	IF	CITATIONS
307	Unique Surface Properties of Nanocomposite Thin Film Photocatalysts of TiO2 and Poly(tetrafluoroethylene). Chemistry Letters, 2015, 44, 509-511.	0.7	8
308	Spherical TiO <sub>2</sub> /Mesoporous SiO <sub>2</sub> Core/Shell Type Photocatalyst for Water Purification. Journal of Nanoscience and Nanotechnology, 2016, 16, 9273-9277.	0.9	8
309	Specific Enhancement of Activity of Carbon-supported Single-site Co Catalyst in the Microwave-assisted Solvent-free Aerobic Oxidation. Chemistry Letters, 2017, 46, 789-791.	0.7	8
310	Non-noble metal doped perovskite as a promising catalyst for ammonia borane dehydrogenation. Catalysis Today, 2020, 351, 6-11.	2.2	8
311	Tunable surface modification of a hematite photoanode by a Co(salen)-based cocatalyst for boosting photoelectrochemical performance. Catalysis Science and Technology, 2020, 10, 1714-1723.	2.1	8
312	Synthesis of small Ni-core–Au-shell catalytic nanoparticles on TiO <sub>2</sub> by galvanic replacement reaction. Nanoscale Advances, 2021, 3, 823-835.	2.2	8
313	Ru complex and N, P-containing polymers confined within mesoporous hollow carbon spheres for hydrogenation of CO2 to formate. Nano Research, 2023, 16, 4515-4523.	5.8	8
314	Experimental and computational study on roles of WOx promoting strong metal support promoter interaction in Pt catalysts during glycerol hydrogenolysis. Scientific Reports, 2021, 11, 530.	1.6	8
315	Dual Active Centers Bridged by Oxygen Vacancies of Ruthenium Singleâ€Atom Hybrids Supported on Molybdenum Oxide for Photocatalytic Ammonia Synthesis. Angewandte Chemie, 2022, 134, .	1.6	8
316	Preparation of Size-controlled Copper-nanoparticle-supported Catalyst Using Rapid and Uniform Heating under Microwave Irradiation. Chemistry Letters, 2012, 41, 614-616.	0.7	7
317	Hydrogenation of 1-octene over skeletal Pd catalysts prepared from Pd–Zr amorphous alloys and the effect of Ni addition. Catalysis Today, 2016, 265, 138-143.	2.2	7
318	Preparation, characterizations, and antibacterial properties of Cu/SnO2 nanocomposite bilayer coatings. Journal of Coatings Technology Research, 2018, 15, 437-443.	1.2	7
319	Design of Advanced Functional Materials Using Nanoporous Single‧ite Photocatalysts. Chemical Record, 2020, 20, 660-671.	2.9	7
320	Catalytic and photocatalytic epoxidation over microporous titanosilicates with nanosheet or layered structure. Catalysis Today, 2021, 376, 28-35.	2.2	7
321	Hybrid Phase MoS <sub>2</sub> as a Noble Metal-Free Photocatalyst for Conversion of Nitroaromatics to Aminoaromatics. Journal of Physical Chemistry C, 2021, 125, 20887-20895.	1.5	7
322	Effect of ion-exchanged alkali metal cations on the photolysis of 2-pentanone included within ZSM-5 zeolite cavities: a study of ab initio molecular orbital calculations. Research on Chemical Intermediates, 2001, 27, 89-102.	1.3	6
323	Thermodynamics and phase diagram calculation of some sections in the Ag-Bi-Sn system. Journal of the Serbian Chemical Society, 2007, 72, 901-909.	0.4	6
324	Synthesis and photocatalytic activity of TiO2 nanoparticles fluorine-modified with TiF4. Research on Chemical Intermediates, 2008, 34, 331-337.	1.3	6

#	Article	IF	CITATIONS
325	Simple Design of Hydrophobic Zeolite Material by Modification Using TEFS and its Application as a Support of TiO2 Photocatalyst. Topics in Catalysis, 2009, 52, 193-196.	1.3	6
326	Design of TiO <sub>2</sub> -loaded Porous Siliceous Materials and Application to Photocatalytic Environmental Purification. Journal of the Japan Petroleum Institute, 2016, 59, 165-173.	0.4	6
327	Dramatically Enhanced Phenol Degradation on Alkali Cationâ€Anchored TiO <sub>2</sub> /SiO <sub>2</sub> Hybrids: Effect of Cationâ€i€ Interaction as a Diffusionâ€Controlling Tool in Heterogeneous Catalysis. ChemistrySelect, 2017, 2, 4332-4337.	0.7	6
328	Preparation of W-Containing Mesoporous Silica Thin Films and Their Surface Hydrophilic Properties. E-Journal of Surface Science and Nanotechnology, 2009, 7, 141-144.	0.1	6
329	Design of Nano-Sized Pt Metals Synthesized on Ti-Containing Mesoporous Silicas and Efficient Catalytic Application for NO Reduction. Materials Transactions, 2008, 49, 398-401.	0.4	5
330	Pt-supported Spherical Mesoporous Silica as a Nanosized Catalyst for Efficient Liquid-Phase Hydrogenation. Topics in Catalysis, 2014, 57, 1026-1031.	1.3	5
331	Reaction Kinetics on Allophane–Titania Nanocomposite Electrodes for Photofuel Cells. Chemistry Letters, 2017, 46, 659-661.	0.7	5
332	Photocatalytic Reaction and Surface Photoreaction on Ultra-Fine Semiconductor Particles. Design of Anchored Molecular Size Photocatalysts for Environmental Applications Hyomen Kagaku, 1995, 16, 194-200.	0.0	5
333	Photocatalytic Epoxidation of Olefins Using Molecular O2by TiO2Incorporated in Hydrophobic Y Zeolite. Rapid Communication in Photoscience, 2015, 4, 19-21.	0.1	5
334	Intrinsic band gap shift in Ti silicalites modified by V ion implantation: Ab initio and density functional theory study. International Journal of Quantum Chemistry, 2004, 96, 349-354.	1.0	4
335	Photoluminescence properties of Ag2S semiconductor clusters synthesized in micropores and mesopores. Research on Chemical Intermediates, 2008, 34, 519-524.	1.3	4
336	Effects of preparation conditions on the synthesis of nano-sized Ag metal particles by the wet-process using 3-mercapto-propionic acid. Research on Chemical Intermediates, 2008, 34, 641-647.	1.3	4
337	Preparation of nano-sized Pt metal particles by photo-assisted deposition (PAD) on transparent Ti-containing mesoporous silica thin film. Research on Chemical Intermediates, 2008, 34, 495-505.	1.3	4
338	New Method for the Synthesis of Ru Nanoparticles Using Photoexcited Fullerene C60-containing Mesoporous Silica as a Catalyst Support. Chemistry Letters, 2015, 44, 1691-1693.	0.7	4
339	Preparation of Titanium Oxide/Activated Carbon Fiber Photocatalysts Using an Ionized Cluster Beam Method. Tanso, 1998, 1998, 296-298.	0.1	4
340	Photocatalytic Approaches for Hydrogen Production via Formic Acid Decomposition. Topics in Current Chemistry Collections, 2020, , 193-223.	0.2	4
341	Improvement of acid resistance of Zn-doped dentin by newly generated chemical bonds. Materials and Design, 2022, 215, 110412.	3.3	4
342	The Photocatalytic Reduction of CO2 with H2O on Titanium Oxide Catalysts Sekiyu Gakkaishi (Journal) Tj ETQ	iq0 0 0 rgB	T /Qverlock 10

20

#	Article	IF	CITATIONS
343	Coating of Transparent Ti-containing Mesoporous Silica Thin Films on Quartz and Aluminum Alloy Substrates for Fabrication of Highly Hydrophilic Surfaces. ISIJ International, 2010, 50, 255-258.	0.6	3
344	Synthesis of SiO2-TiO2 fibers with photocatalytic activity by TiCl4 vapor curing on melt-spun silicone resin fiber. Journal of the Ceramic Society of Japan, 2011, 119, 544-547.	0.5	3
345	Design and Functionalization of Photocatalytic Systems within Mesoporous Silica. ChemSusChem, 2014, 7, 1495-1495.	3.6	3
346	Poly(ethyleneimine)-tethered Ir Complex Catalyst Immobilized in Titanate Nanotubes for Hydrogenation of CO2 to Formic Acid. ChemCatChem, 2017, 9, 1867-1867.	1.8	3
347	Single-Site Heterogeneous Catalysts and Photocatalysts for Emerging Applications. ACS Symposium Series, 2020, , 151-188.	0.5	3
348	Mesoporous silica–supported Ag-based plasmonic photocatalysts. , 2020, , 353-368.		3
349	PdAg Nanoparticles Supported on an Amine-functionalized MOF as a Photo-switchable Catalyst for Hydrogen Storage/Delivery Mediated by CO2/Formic Acid. Chemistry Letters, 2021, 50, 607-610.	0.7	3
350	Hydrodeoxygenation of Aromatic Ketones under Mild Conditions over Pd-loaded Hydrogen Molybdenum Bronze with Plasmonic Features. Chemistry Letters, 2022, 51, 166-169.	0.7	3
351	Effect of metal deposition on the photocatalytic activity of titania-silica for the removal of 2-propanol diluted in water. Research on Chemical Intermediates, 2009, 35, 305-312.	1.3	2
352	Semiconductorâ€based Photoanodes Modified with Metalâ€Organic Frameworks and Molecular Catalysts as Cocatalysts for Enhanced Photoelectrochemical Water Oxidation Reaction. ChemCatChem, 2021, 13, 5058-5072.	1.8	2
353	Size effects in plasmonic gold nanorod based Pd-rGO hybrid catalyst for promoting visible-light-driven Suzuki-Miyaura coupling reaction. Catalysis Today, 2022, , .	2.2	2
354	Development of Multi-functional Catalysts for Capture and Catalytic Transformation of Carbon Dioxide Using Nanoporous Materials. Journal of the Japan Petroleum Institute, 2022, 65, 125-133.	0.4	2
355	XAFS Study on Nano-Sized Pd Metal Catalyst Deposited on Ti-Containing Zeolite by a Photo-Assisted Deposition (PAD) Method. AIP Conference Proceedings, 2007, , .	0.3	1
356	Degradation of organic compounds on TiO2 photocatalysts prepared by a hydrothermal method in the presence of NH4F. Research on Chemical Intermediates, 2009, 35, 299-304.	1.3	1
357	Tetragonal Distortion in Thermochromic Copper(II) Diamine Complex Induced by the Fixation on Silica Surfaces and Their Catalytic Investigations. Topics in Catalysis, 2009, 52, 586-591.	1.3	1
358	Hydrogenation of Phenol Using Silica-Supported Pd and PdAu Catalysts in the Presence of H2 and O2. Bulletin of the Chemical Society of Japan, 2012, 85, 1057-1059.	2.0	1
359	Environmental Transmission Electron Microscopy Study of Diesel Carbon Soot Combustion under Simulated Catalyticâ€Reaction Conditions. ChemPhysChem, 2015, 16, 1321-1321.	1.0	1
360	PdAu Core–Shell Nanostructures as Visible-Light Responsive Plasmonic Photocatalysts. Nanostructure Science and Technology, 2021, , 261-274.	0.1	1

#	Article	IF	CITATIONS
361	Control of Photochemical and Photocatalytic Reactions in Zeolite Micro-Cavities Hyomen Kagaku, 1996, 17, 270-275.	0.0	0
362	Synthesis of a Fe-Ni Alloy on a Ceria Support as a Noble-Metal-Free Catalyst for Hydrogen Production from Chemical Hydrogen Storage Materials. ChemCatChem, 2015, 7, 1235-1235.	1.8	0
363	Design and Applications of Single-Site Photocatalysts Using Nano-Space. Bulletin of Japan Society of Coordination Chemistry, 2017, 69, 35-44.	0.1	0
364	Synthesis of Plasmonic Catalyst with Core-Shell Structure for Visible Light Enhanced Catalytic Performance. Nanostructure Science and Technology, 2021, , 233-243.	0.1	0
365	Design and Synthesis of Yolk–Shell Nanostructured Silica Encapsulating Metal Nanoparticles and Aminopolymers for Selective Hydrogenation Reactions. Nanostructure Science and Technology, 2021, , 395-411.	0.1	0
366	Design of Plasmonic Catalysts Utilizing Nanostructures. Journal of the Japan Petroleum Institute, 2021, 64, 155-165.	0.4	0
367	Supported Core–Shell Alloy Nanoparticle Catalysts for the Carbon Dioxide Hydrogenation to Formic Acid. Nanostructure Science and Technology, 2021, , 151-163.	0.1	0
368	Hollow Carbon Spheres Encapsulating Metal Nanoparticles for CO2 Hydrogenation Reactions. Nanostructure Science and Technology, 2021, , 425-440.	0.1	0
369	Metal Catalysts for Storage and Delivery of Hydrogen Energy. Materia Japan, 2017, 56, 653-659.	0.1	0
370	Chemical Hydrogen Storage and Release Driven by PdAg Alloy Nanoparticle Catalysts. Materia Japan, 2020, 59, 361-365.	0.1	0